Arthritis Research & Therapy

RESEARCH

Open Access

Unraveling the role of lncRNAs and their associated nearby coding genes in the pathogenesis of systemic lupus erythematosus

Tao Liu[1], Mingyue Yang[2], Xiunan Feng[1], Xiaojuan Zou[1], Ying Xia[2], Lu Chen[1], Zixin Gao[1], Ling Zhao[1*] and Xiaosong Wang[2*]

Abstract

Background The role of long non-coding RNAs (lncRNAs) and their nearby messenger RNAs (mRNAs) in systemic lupus erythematosus (SLE) pathogenesis is not well understood.

Method High-throughput sequencing was utilized to analyze PBMCs obtained from SLE patients. Subsequently, we conducted differential analysis, Gene Ontology (GO) analysis, Kyoto Encyclopedia of Genes and Genomes (KEGG) analysis, and verification through quantitative real-time PCR (qRT-PCR). Additionally, qRT-PCR was used to analyze the levels of lncRNAs or mRNAs in transfected Raji cells.

Results We identified 419 differentially expressed (DE) lncRNAs and their 337 nearby DE mRNAs in SLE patients. More than 67% of the DE lncRNAs were lincRNAs and intronic_lncRNAs. The most significantly regulated nearby mRNAs in SLE patients were *LTF* and *CIRBP*, potentially involved in recurrent infection and photosensitivity. GO analysis revealed upregulation of the immune effector process term, with genes such as *C1qA*, *C1qC*, *C1qB*, *NLRP3*, and *CXCL6* participating in this term and the upregulated pertussis signaling pathway. Analysis of the nearby coding genes of 88 lincRNAs indicated that *XLOC_185773* had the highest number of nearby encoding genes and was negatively correlated with peripheral blood lymphocyte counts, potentially regulating *HARS*. Furthermore, *LNC_005556*, an antisense DE lncRNA, was negatively correlated with lupus nephritis occurrence and may regulate the upregulated *IGLL5* in patients.

Conclusions The current study provides insights into the dysregulation of lncRNAs and nearby mRNAs in SLE, highlighting potential key players in the pathogenesis of the disease.

Keywords High-throughput sequencing, Long non-coding RNA, Nearby coding genes, Peripheral blood mononuclear cells, Systemic lupus erythematosus

*Correspondence:
Ling Zhao
zhaoling17@jlu.edu.cn
Xiaosong Wang
xiaosongwang@jlu.edu.cn

[1]Department of Rheumatology and Immunology, The First Hospital of Jilin University, Changchun 130021, China
[2]Department of Translational Medicine, The First Hospital of Jilin University, Changchun 130021, China

Background

Systemic lupus erythematosus (SLE) is an autoimmune disease that damages various organs in the body, resulting in high morbidity and mortality [1]. The pathogenesis of SLE involves different factors, such as environmental factors, viral infections, autoantibodies, complement, and immune complex deposition. Ultraviolet radiation causes DNA damage, cell stress response, apoptosis, and increases the production of autoantigens [2]. Viral infections not only activate innate and interferon-related immune responses but also participate in the pathogenesis of SLE through molecular simulation and epitope diffusion [3, 4]. Moreover, abnormal activation of the autoimmune system occurs due to altered apoptosis or debris clearance-related gene expression [5]. Complement changes, including *C1q*, *C2*, and *C4A*, are also involved in SLE [6].

Long noncoding RNAs (lncRNAs) are a type of noncoding RNA that, ranging in length from 200 nt to over 100 kb. They are located in extended or overlapping antisense transcripts between protein-coding genes and usually lack an obvious open reading frame. LncRNA have attracted increasing attention due to their participation in the pathogenesis of many diseases [7–9]. Cis-regulation refers to the functional relationship between lncRNAs and their neighboring protein-coding genes. When lncRNAs are located within 100 kb upstream or downstream of a gene, they may interact with mRNA to participate in transcriptional regulation [10, 11]. There are three modes of action for these lncRNAs: (1) binding to chromatin or DNA strands to affect transcription and mRNA splicing, (2) affecting the binding of transcription factors to promoter and enhancer regions, and (3) binding to transcription elements to affect gene transcription and expression. It was reported that lncRNA may enhance the production of *IFN-γ* by cis regulating *LMBRD2* and thereby exacerbating SLE [12]. Several other interaction pairs of lncRNA-nearby targeted mRNA were identified in SLE [13]. Therefore, lncRNAs and their nearby mRNAs are involved in the pathogenesis of SLE.

In the current study, we detected the expression profiles of lncRNAs in the PBMCs of SLE patients using high-throughput sequencing and further analyzed the specific lncRNAs and their nearby mRNAs in SLE patients. We predicted the biological functions of the differentially expressed (DE) lncRNAs in SLE by performing GO and KEGG analysis of their nearby DE mRNAs. Research on the pathogenic genes helps us to better understand the pathogenesis of SLE and provides evidence for new approaches to the treatment of SLE.

Methods

Patient data and sample collection

We obtained clinical data from 50 SLE patients who received treatment at the First Hospital of Jilin University between August 2018 and October 2019 (Additional file 1). The diagnostic criteria for SLE were based on the American College of Rheumatology (ACR) guidelines established in 1997, which require meeting at least 4 of 11 criteria for systemic lupus erythematosus. Sample collection was conducted after the patients' admission and prior to the initiation of drug therapy. Clinical information such as the disease course of the patients and whether there is associated lupus nephritis can be found in Additional file 2. We included 40 healthy subjects of similar age and sex as the control group. We performed a detailed analysis of the age and sex distribution for both SLE patients and the healthy control group (Additional file 3). Among the collected samples, the peak age of onset for SLE patients was 21 to 30 years old. The patients were mainly female, and the proportion of females among patients in all age groups was higher than 91.7%. The age and sex distribution of the healthy control group was matched with that of the SLE patient group to ensure there was no significant difference between the two groups in terms of age and sex. All patients and healthy controls had no alcoholism, viral carcinogenesis, malaria, or cancer at the time of sample collection, and those with current or recent infections were excluded. Peripheral blood mononuclear cells (PBMCs) from 20 SLE patients and 10 healthy subjects were randomly selected for high-throughput sequencing, while PBMCs from other SLE patients and healthy subjects were used for validation assays.

Ethics statement

This study was approved by the Institutional Medical Ethics Review Board of the First Hospital of Jilin University (reference number: 2017-087), and all procedures were conducted in accordance with the Declaration of Helsinki.

High-throughput sequencing

RNA purity and integrity were assessed as previously described [14–16]. Three micrograms of RNA per sample were used for sample preparation. Sequencing was performed as previously described [16]. Briefly, ribosomal RNA was removed using the EpicentreRibo-zero™ rRNA Removal Kit (Epicenter, USA), and rRNA-free residues were cleaned up by ethanol precipitation. Subsequently, sequencing libraries were generated using the NEBNext® Ultra™ Directional RNA Library Prep Kit (NEB, USA) following the manufacturer's instructions. The quality of the sequencing library was assessed using an Agilent

Bioanalyzer 2100 system. Finally, sequencing was performed on an Illumina HiSeq X Ten (paired-end 150-bp reads).

Sequencing data analysis

Sequencing analysis was performed as previously described [16]. Briefly, the reference genome and gene model annotation files were downloaded from the genome website (Homo_sapiens.GRCh38.94). The index of the reference genome was built, and the paired-end clean reads were aligned to the reference genome using HISAT2 v2.0.4 [17]. HISAT2 was run with '--RNA-strandness RF', and other parameters were set as default. The FPKMs of both lncRNAs and coding transcripts in each sample were calculated using StringTie (v2.1.1) [18]. FPKM was calculated based on the length of the fragments and read count mapped to this fragment, and represents fragments per kilobase of exon per million fragments mapped.

To explore the transcriptome assembly, we utilized the ballgown suite, which allowed for interactive visualization of transcript structures and feature-specific abundances for each locus. Additionally, posthoc annotation of assembled features to annotated features was performed [19]. We investigated the cis role of long non-coding RNAs (lncRNAs) by searching for coding genes located 100 kb upstream and downstream of the lncRNAs, and analyzing their functions. The differential expression of replicated count data was examined using edgeR (3.0.8), a Bioconductor software package. Transcripts with a corrected p-value less than 0.05 were assigned as DE. An overdispersed Poisson model was used to account for biological and technical variability. GO enrichment analysis and KEGG analysis were performed as previously described [14, 15].

Quantitative real-time PCR (qRT-PCR)

Total RNA was extracted from cells stored at -80 ℃ (per 5×10^6 cells/ml) in TRIzol reagent (Invitrogen, Carlsbad, CA, USA), and qRT-PCR was performed as previously described [20]. The primer sequences are listed in Additional file 4.

Cell culture and transfection

Raji cells were cultured overnight in 24-well plates at a density of 5×10^5 cells/well in 1 ml of RPMI1640 medium (Corning, NY, USA) supplemented with 10% fetal bovine serum (ZQXZBIO, Shanghai, China). Small interference RNAs targeting *XLOC_185773* (si-XLOC_185773) and *LNC_005556* (si-LNC_005556), along with negative controls (si-Control), were procured from IBSBIO (Shanghai, China). The si-XLOC_185773 or si-LNC_005556 were transfected into the cells at a functional concentration of 50 nM using Lipofectamine 3000 (Invitrogen, CA, USA, 2 ul/well). Non-transfected cells served as controls. Post 48 h of transfection, cells were stimulated with lipopolysaccharide (LPS, Solarbio, Beijing, China, 10 ng/ml) for 4 h, with cells devoid of LPS serving as controls. Subsequently, cells from each well were harvested and preserved in 1 ml of TRIZOL for qRT-PCR analysis.

Statistical analysis

Statistical analysis and graph rendering were performed using GraphPad Prism 8.0 (GraphPad Software, San Diego CA, USA). An unsupervised heatmap was generated using all data between the maximum (red) and minimum (blue) values for each gene to compare different matrices. The Wilcoxon signed-rank test for paired samples and Mann-Whitney U test for unpaired samples were applied, with a p-value less than 0.05 considered statistically significant.

Results

Differential expression analysis of LncRNAs in PBMCs of SLE patients

We conducted a comprehensive analysis of the expression profiles of lncRNAs in PBMCs obtained from SLE patients and healthy controls (Fig. 1A). The volcano plots depicted the distribution of significantly up or downregulated lncRNA genes (Fig. 1B). The clustering analysis of DE lncRNAs is presented in Fig. 1C. Using a cutoff of $|\text{foldchange}| > 2$ and p-value < 0.05, we identified 419 DE lncRNAs, of which 241 were upregulated (length and fold change ranged from 215 to 287,306 and 0.9 to 10.07, respectively) and 178 were downregulated (length and fold change ranged from 282 to 204,537 and 0.85 to 9.21, respectively) (Fig. 1D). The number of dysregulated lncRNAs varied among the subgroups with different fold changes, with most of the lncRNAs falling in the $0 \leq$ fold change < 2 and the $2 \leq$ fold change < 4 subgroups (Fig. 1E). According to the annotation file (http://ftp.ensembl.org/pub/release-94/gtf/homo_sapiens/) of the genome (http://ftp.ensembl.org/pub/release-94/fasta/homo_sapiens/ncrna/), the gene sources of differential lncRNAs are classified into 8 categories: lincRNA, intronic_lncRNA, antisense_lncRNA, processed_transcript, TEC, sense_intronic, sense_overlapping, and misc_RNA. Notably, more than 67% of the dysregulated lncRNAs belonged to the lincRNA and intronic_lncRNA groups, regardless of whether the lncRNAs were upregulated (Fig. 1F) or downregulated (Fig. 1G). Furthermore, we identified the top 10 distinctly regulated lncRNAs, including the most upregulated lncRNA, *LNC_005556* (fold change, 10.07), and the most downregulated lncRNA, *LNC_000099* (fold change, 9.21), as shown in Fig. 1H. These lncRNAs may contribute to the pathogenesis of SLE.

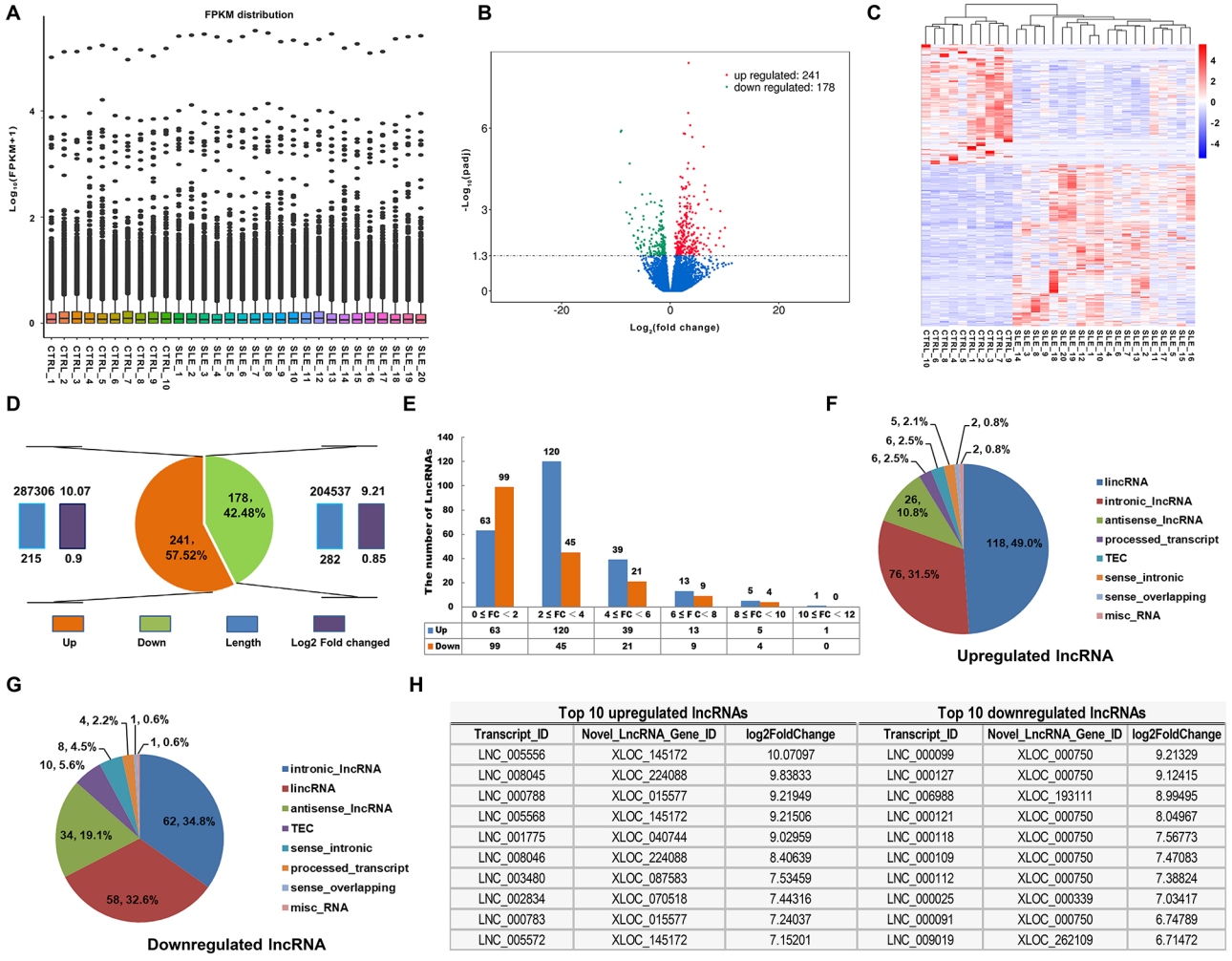

H

Top 10 upregulated lncRNAs			Top 10 downregulated lncRNAs		
Transcript_ID	Novel_LncRNA_Gene_ID	log2FoldChange	Transcript_ID	Novel_LncRNA_Gene_ID	log2FoldChange
LNC_005556	XLOC_145172	10.07097	LNC_000099	XLOC_000750	9.21329
LNC_008045	XLOC_224088	9.83833	LNC_000127	XLOC_000750	9.12415
LNC_000788	XLOC_015577	9.21949	LNC_006988	XLOC_193111	8.99495
LNC_005568	XLOC_145172	9.21506	LNC_000121	XLOC_000750	8.04967
LNC_001775	XLOC_040744	9.02959	LNC_000118	XLOC_000750	7.56773
LNC_008046	XLOC_224088	8.40639	LNC_000109	XLOC_000750	7.47083
LNC_003480	XLOC_087583	7.53459	LNC_000112	XLOC_000750	7.38824
LNC_002834	XLOC_070518	7.44316	LNC_000025	XLOC_000339	7.03417
LNC_000783	XLOC_015577	7.24037	LNC_000091	XLOC_000750	6.74789
LNC_005572	XLOC_145172	7.15201	LNC_009019	XLOC_262109	6.71472

Fig. 1 LncRNA expression profiles in PBMCs of SLE patients. (**A**) Boxplot depicting the distribution of FPKM values for lncRNAs in each sample. (**B**) Volcano plot displaying the differentially expressed (DE) lncRNAs between the SLE and control groups. Each point represents a detectable gene in both groups. (**C**) Cluster analysis of 419 differentially expressed (DE) lncRNAs between the SLE and control groups with an adjusted p-value < 0.05. (**D**) Pie chart showing the number of upregulated and downregulated lncRNAs with respect to length and fold change. (**E**) Number of lncRNAs in different subgroups classified by fold change (FC). (**F** and **G**) Pie chart showing the classification of upregulated (**F**) and downregulated (**G**) lncRNAs including lincRNA, intronic_lncRNA, antisense_lncRNA, processed_transcript, TEC, sense_intronic, sense_overlapping, and misc_RNA. (**H**) Top 10 significantly upregulated or downregulated lncRNAs

The nearby DE mRNA profiles in PBMCs of SLE patients

To further investigate the potential functional roles of DE lncRNAs, we analyzed the DE lncRNA-associated nearby DE mRNAs in the PBMCs from SLE patients compared to that from healthy controls (Fig. 2A). The volcano plots showed the number and distribution of significantly up or downregulated nearby mRNA genes (Fig. 2B). Clustering analysis results of nearby DE mRNA were presented in Fig. 2C. Using |fold change| cutoff > 2.0 and p-value cutoff < 0.05, we identified a total of 234 mRNAs with upregulated expression and 103 mRNAs with downregulated expression among the 337 DE mRNAs (Fig. 2D). The length and fold change of these mRNAs ranged from 598 to 633,422 and 0.77 to 11.59, respectively. Similar to the lncRNAs, most dysregulated mRNAs were in the 0 ≤ fold change < 2 subgroup and the 2 ≤ fold change < 4 subgroup (Fig. 2E). Furthermore, we identified the top 10 DE mRNAs, with *LTF* (ENST00000417439; fold change, 11.59) being the most significantly upregulated mRNA and *CIRBP* (ENST00000586548; fold change, 8.87) being the most significantly downregulated mRNA (Fig. 2F).

Gene ontology (GO) analysis of the nearby DE mRNAs in PBMCs of SLE patients compared to healthy controls

To gain insights into the biological processes, cellular components, and molecular functions associated with SLE, we performed a comprehensive GO analysis of the nearby DE mRNAs identified in PBMCs of SLE patients compared to healthy controls. Our analysis revealed the top 10 significantly enriched terms, as shown in the pie

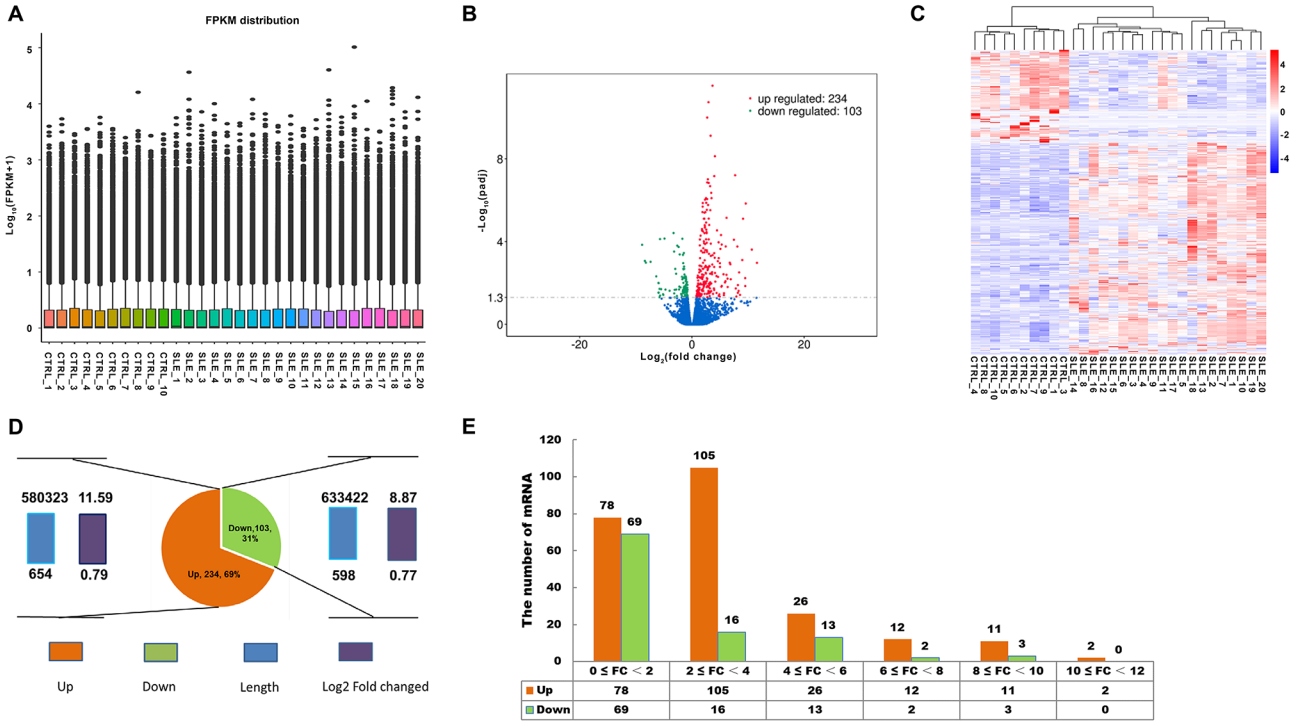

F

Top 10 upregulated nearby mRNAs of DE lncRNAs				Top 10 downregulated nearby mRNAs of DE lncRNAs			
mRNA_ID	mRNA_Gene_ID	mRNA_Gene_Symbol	log2FoldChange	mRNA_ID	mRNA_Gene_ID	mRNA_Gene_Symbol	log2FoldChange
ENST00000417439	ENSG00000012223	LTF	11.58675	ENST00000586548	ENSG00000099622	CIRBP	8.86839
ENST00000647020	ENSG00000244734	HBB	10.67316	ENST00000457599	ENSG00000117713	ARID1A	8.37564
ENST00000373836	ENSG00000204138	PHACTR4	9.59335	ENST00000644671	ENSG00000197912	SPG7	8.19798
ENST00000620366	ENSG00000122203	KIAA1191	9.50760	ENST00000610735	ENSG00000153094	BCL2L11	7.36397
ENST00000398905	ENSG00000157554	ERG	9.49116	ENST00000418590	ENSG00000100241	SBF1	6.34847
ENST00000351231	ENSG00000164045	CDC25A	9.11109	ENST00000452774	ENSG00000131480	AOC2	5.94300
ENST00000422444	ENSG00000197121	PGAP1	8.97170	ENST00000542322	ENSG00000155324	GRAMD2B	5.93402
ENST00000556506	ENSG00000100902	PSMA6	8.57519	ENST00000263437	ENSG00000022556	NLRP2	5.93045
ENST00000370757	ENSG00000122420	PTGFR	8.41339	ENST00000569879	ENSG00000162066	AMDHD2	5.92629
ENST00000527275	ENSG00000166311	SMPD1	8.31852	ENST00000502499	ENSG00000015479	MATR3	5.78336

Fig. 2 Nearby differentially expressed (DE) mRNA profiles in PBMCs of SLE patients. (**A**) Boxplot showing the FPKM distribution of nearby mRNAs in each sample. (**B**) Volcano plot displaying the nearby DE mRNAs between the SLE and control groups. Each point represents a detectable gene in both groups. (**C**) Cluster analysis of 337 nearby DE mRNAs between the SLE and control groups with an adjusted p-value < 0.05. (**D**) Pie chart showing the number of upregulated and downregulated mRNAs with respect to length and fold change. (**E**) Number of mRNAs in different subgroups classified by fold change (FC). (**F**) Top 10 significantly upregulated or downregulated mRNAs

chart (Figs. 3A, D and G and 4A and D, and 4G), and the top 10 enrichment scores and fold values, as shown in the bar plot (Figs. 3B, E and H and 4B and E, and 4H) and (Figs. 3C, F and I and 4C and F, and 4I), respectively. Our findings suggest that immune effector processes, defense responses, and metabolic processes are likely involved in SLE pathogenesis. Specifically, upregulated mRNAs were enriched in GO terms related to immune effector processes, defense responses, and responses to external biotic stimuli (Fig. 3B), while downregulated mRNAs were enriched in GO terms related to negative regulation of viral RNA replication, DNA cytosine deamination, and mannose metabolic process (Fig. 4B). The detailed GO terms and their descriptions can be found in Additional file 5–10.

Pathway analysis of the nearby DE mRNAs in PBMCs of SLE patients compared to healthy controls

Pathway analysis is a functional analysis that involves mapping genes to Kyoto Encyclopedia of Genes and Genomes (KEGG) pathways. Our analysis revealed that there were 18 upregulated and 14 downregulated pathways in SLE patients compared to healthy controls (Fig. 5A). The bar plot displayed the scores (-log10 (p-value)) of the top 10 significantly enriched pathways (Fig. 5B and D). As shown in Fig. 5B-C our findings

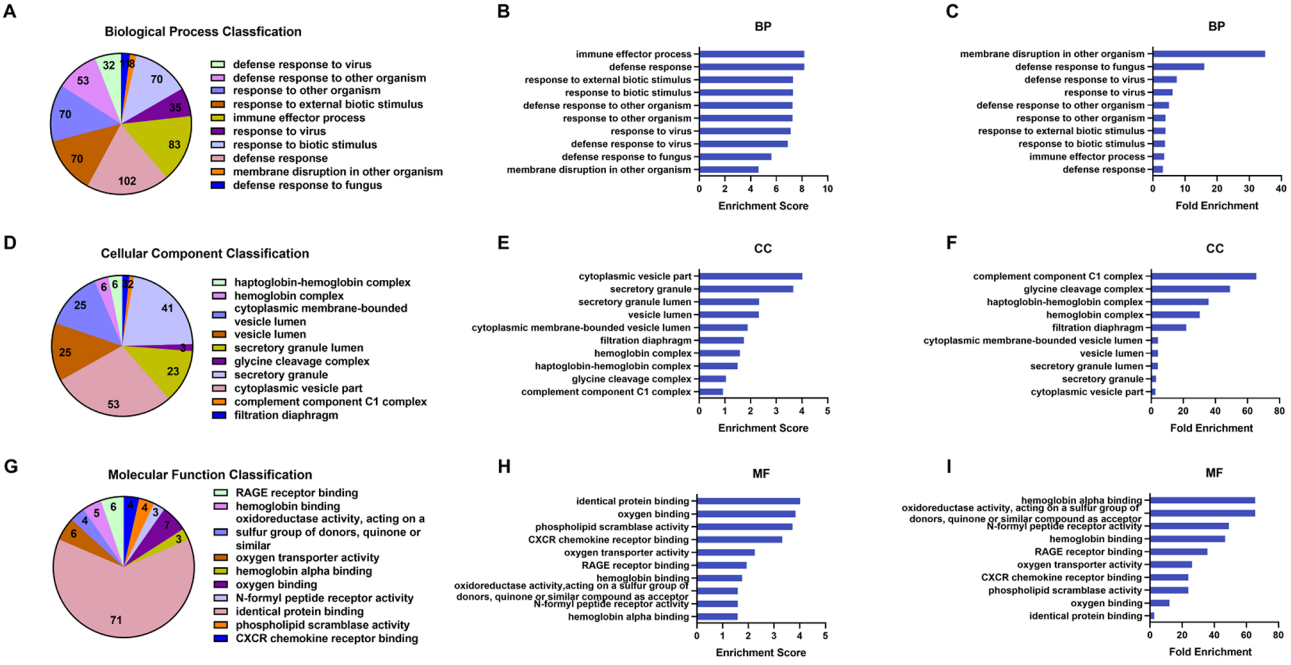

Fig. 3 Gene Ontology (GO) analysis of upregulated nearby mRNAs. (**A**, **D**, and **G**) The pie chart displays the top 10 significant enrichment terms for biological process (BP), cellular component (CC), and molecular function (MF), respectively. (**B**, **E**, and **H**) The bar plot shows the top 10 enrichment scores (-log10 (p-value)) for BP, CC, and MF, respectively. (**C**, **F**, and **I**) The bar plot shows the top 10 fold enrichment values ((count/pop. hits)/ (list. total/pop. total)) for BP, CC, and MF, respectively. The term "count" refers to the number of differentially expressed (DE) genes associated with the listed ID of the gene ontology term, while "pop. hits" refers to the number of background population genes associated with the listed ID of the gene ontology term. "List. Total" represents the total number of DE genes, and "Pop. Total" represents the total number of background population genes

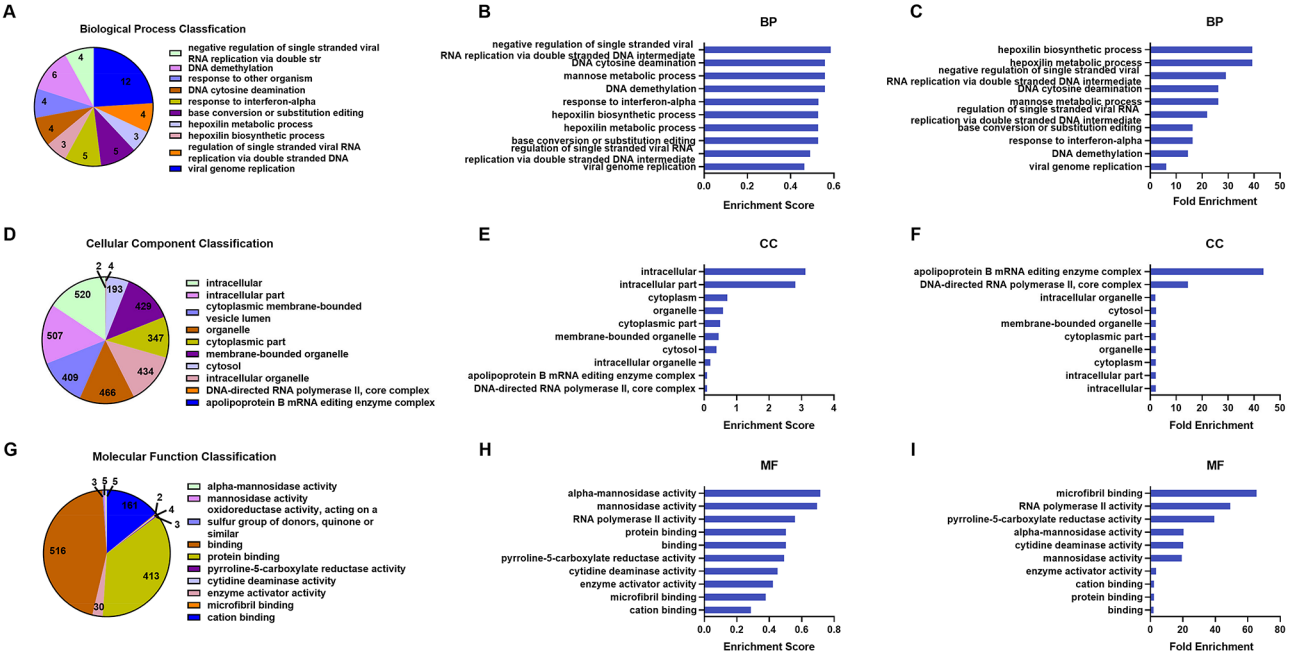

Fig. 4 Gene Ontology (GO) analysis of downregulated nearby mRNAs. (**A**, **D**, and **G**) The pie chart displays the top 10 significant enrichment terms for biological process (BP), cellular component (CC), and molecular function (MF), respectively. (**B**, **E**, and **H**) The bar plot shows the top 10 enrichment scores (-log10 (p-value)) for BP, CC, and MF, respectively. (**C**, **F**, and **I**) The bar plot shows the top 10 fold enrichment values ((count/pop. hits)/ (list. total/pop. total)) for BP, CC, and MF, respectively. The term "count" refers to the number of differentially expressed (DE) genes associated with the listed ID of the gene ontology term, while "pop. hits" refers to the number of background population genes associated with the listed ID of the gene ontology term. "List. Total" represents the total number of DE genes, and "Pop. Total" represents the total number of background population genes

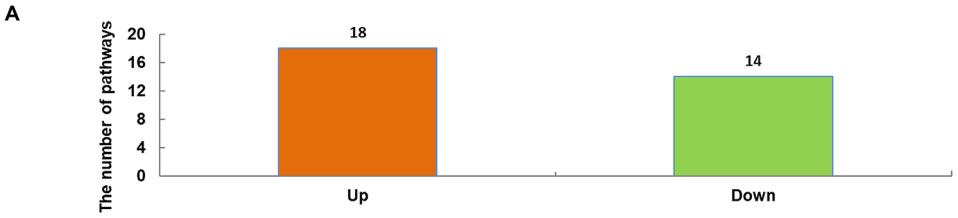

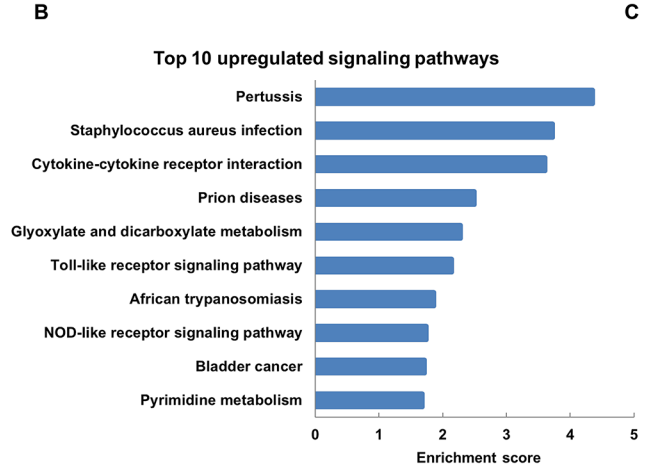

C

Top 10 upregulated signaling pathways

Term	ID	Input number	Background number	P-Value	Corrected P-Value
Pertussis	hsa05133	10	75	4.46E-05	0.00874
Staphylococcus aureus infection	hsa05150	8	57	0.00019	0.01604
Cytokine-cytokine receptor interaction	hsa04060	18	265	0.00024	0.01604
Prion diseases	hsa05020	5	36	0.00318	0.15594
Glyoxylate and dicarboxylate metabolism	hsa00630	4	25	0.00527	0.20644
Toll-like receptor signaling pathway	hsa04620	8	106	0.00718	0.23468
African trypanosomiasis	hsa05143	4	34	0.01377	0.36871
NOD-like receptor signaling pathway	hsa04621	5	57	0.01808	0.36871
Bladder cancer	hsa05219	4	38	0.01934	0.36871
Pyrimidine metabolism	hsa00240	7	105	0.02072	0.36871

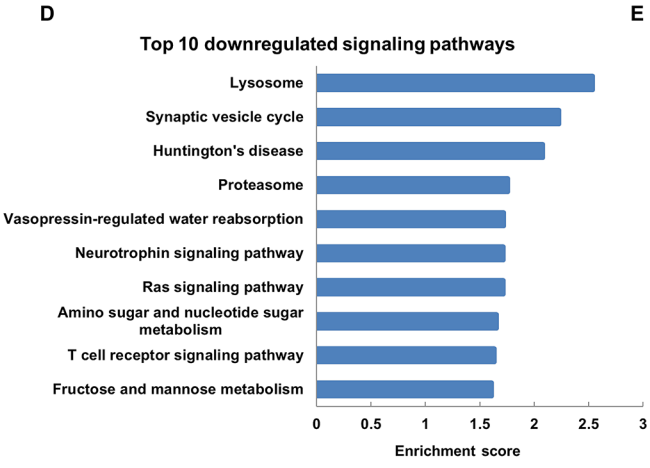

E

Top 10 downregulated signaling pathways

Term	ID	Input number	Background number	P-Value	Corrected P-Value
Lysosome	hsa04142	11	122	0.00291	0.52565
Synaptic vesicle cycle	hsa04721	7	63	0.00591	0.52565
Huntington's disease	hsa05016	13	183	0.00837	0.52565
Proteasome	hsa03050	5	44	0.01751	0.52565
Vasopressin-regulated water reabsorption	hsa04962	5	45	0.01898	0.52565
Neurotrophin signaling pathway	hsa04722	9	120	0.01922	0.52565
Ras signaling pathway	hsa04014	14	228	0.01930	0.52565
Amino sugar and nucleotide sugar metabolism	hsa00520	5	47	0.02214	0.52565
T cell receptor signaling pathway	hsa04660	8	104	0.02335	0.52565
Fructose and mannose metabolism	hsa00051	4	32	0.02461	0.52565

Fig. 5 KEGG analysis of nearby differentially expressed (DE) mRNAs with dysregulated expression. (**A**) The number of pathways for nearby DE mRNAs with dysregulated expression ($p < 0.05$) is shown in a bar chart. (**B**, **C**) Pathway analysis was performed on the upregulated transcripts. (**D**, **F**) Pathway analysis was performed on the downregulated transcripts

indicated that the upregulated mRNAs were mainly involved in pathways related to pertussis (Additional file 11), staphylococcus aureus infection, and cytokine-cytokine receptor interaction. In contrast, as shown in Fig. 5D-E, the downregulated mRNAs were mainly involved in pathways related to lysosome, synaptic vesicle cycle, and Huntington's disease. Pertussis pathway is related to inflammation, and Huntington's disease pathway is related to apoptosis.

qRT-PCR validates the sequencing data of some DE LncRNAs and DE mRNAs

To validate the differential expression of some lncRNAs and mRNAs, we performed qRT-PCR (Fig. 6). Our results showed that the lncRNAs *RP11-1D12.2*, *RP1-249H1.4*, and *CTB-43E15.3* were significantly upregulated, while *RP11-517I3.1*, *RP11-458F8.4*, and *RP11-33E12.2* were significantly downregulated in SLE patients (Fig. 6A-F). Additionally, the mRNAs *LTF*, *HBB*, and *PHACTR4* were significantly upregulated, while *CIRBP*, *ARID1A*, and *SPG7* were significantly downregulated in SLE patients

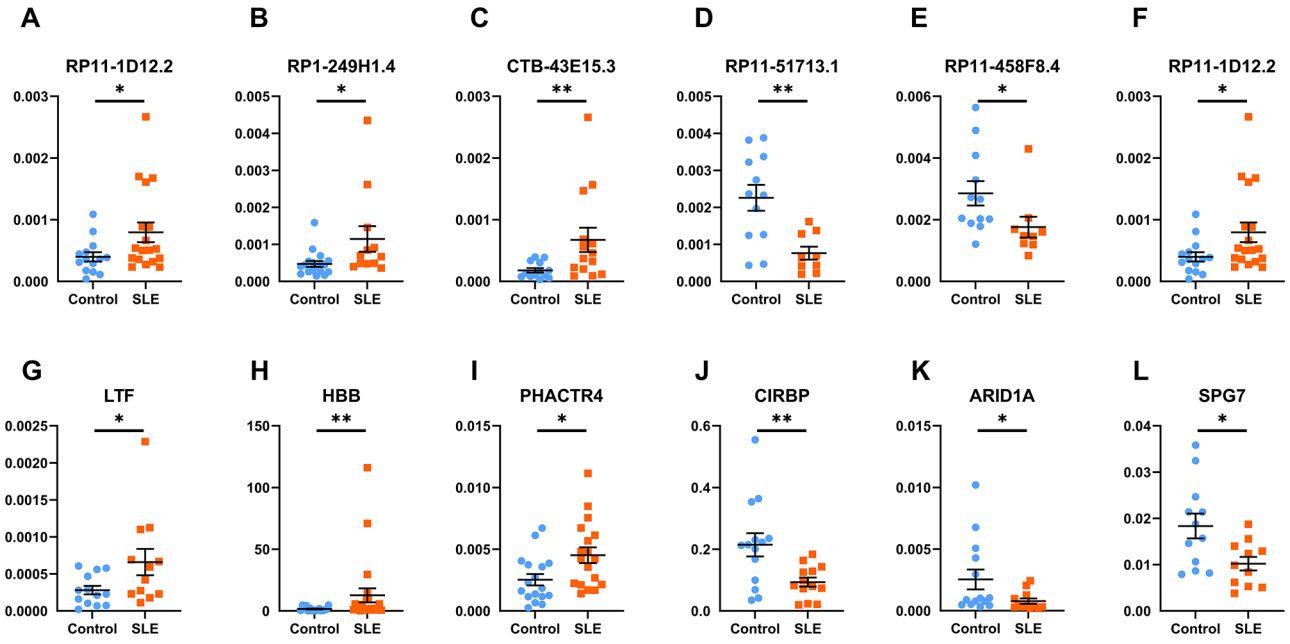

Fig. 6 Validation of differentially expressed (DE) lncRNAs and DE mRNAs by qRT-PCR. (**A**-**F**) The expression levels of three upregulated and three downregulated lncRNAs were validated by qRT-PCR. (**G**-**L**) The expression levels of three upregulated and three downregulated nearby mRNAs were detected by qRT-PCR. $^{**}p < 0.01$, $^{*}p < 0.05$

(Fig. 6G-L). These findings were consistent with the results of our high-throughput sequencing analysis, indicating the reliability of our sequencing data.

Analysis of DE LincRNAs /antisense DE LncRNAs and their nearby DE mRNAs

Given the critical role of long intergenic noncoding RNAs (lincRNAs) in regulating nearby genes, we conducted an analysis of DE lincRNAs. Our analysis revealed a total of 88 DE lincRNAs, with lengths and fold changes ranging from 361 to 287,306 and from 0.85 to 6.97, respectively. Of these, 71 were upregulated and 17 were downregulated (Fig. 7A). Notably, *XLOC_185773* (LncRNA transcript id: *LNC_004051*) had the most nearby mRNAs (Fig. 7B). Further analysis of the nearby mRNAs of *XLOC_185773* revealed that *HARS* was significantly upregulated in SLE patients, and *HARS* levels were positively correlated with *XLOC_185773* levels (Additional file 12). The top 10 lincRNAs, according to fold change, and their nearby mRNAs are shown in Fig. 7C.

Antisense lncRNAs play a regulatory role in the transcriptional or posttranscriptional regulation of corresponding sense mRNAs, thereby exerting their biological functions [21]. Our analysis identified 60 human antisense DE lncRNAs, with lengths and fold changes ranging from 503 to 167,760 and from 0.91 to 10.07, respectively (Fig. 7D). Of these, 26 were upregulated and 34 were downregulated. The top 10 antisense DE lncRNAs and their associated coding genes are displayed in Fig. 7E. *LNC_005556* is the most significantly upregulated antisense lncRNA in SLE, and its nearby mRNA *IGLL5* is also found upregulated in SLE. Further analysis revealed that *IGLL5* levels were positively correlated with *LNC_005556* levels (Additional file 13). Based on the single-cell sequencing results of human PBMCs, *IGLL5* is mainly expressed on human B cell-subsets (Additional file 14). Therefore, we chose Raji cells, a cell line of human B cell origin, for further studies.

XLOC_185773 regulates its nearby coding gene *HARS* level and *Lnc_005556* regulates its nearby coding gene *IGLL5* level

To evaluate the mechanism of specific lncRNAs and their associated nearby coding genes in SLE progression, we first detected the expression patterns of lncRNAs and their associated nearby coding genes in LPS-induced Raji cell model. As the same as we observed in SLE patients, *XLOC_185773*, *HARS*, *LNC_005556*, *IGLL5*, *LNC_008045*, *IFI44L*, *LNC_000788*, *IFI44*, *LNC_001775*, and *IFITM1* were upregulated in LPS-induced Raji cell models (Fig. 8A). To evaluate the exact effect of specific lncRNAs and their associated nearby coding genes in SLE, we knocked down *XLOC_185773*, or *LNC_005556* by small interference RNA. We found that knockdown of lncRNA *XLOC_185773* significantly decreased mRNA levels of HARS in Raji cells upon LPS stimulation (Fig. 8B), indicating that the role of *HARS* in SLE may dependent on *XLOC_185773*. In addition, *LNC_005556* knockdown decreased the levels of its associated nearby coding genes *IGLL5* (Fig. 8C), indicating that the role of

A

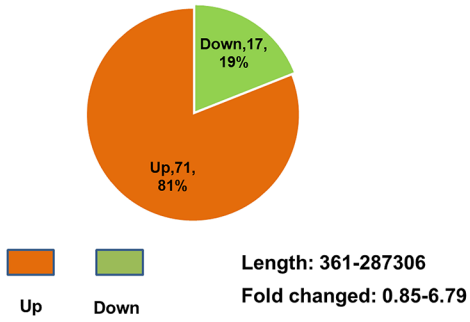

B

LincRNA with the most nearby DE mRNAs

LncRNA_Gene_ID	LncRNA_Gene_Symbol	mRNA_Gene_Id	mRNA_Gene_Symbol	Location
XLOC_185773	--	ENSG00000113108	APBB3	upstream
XLOC_185773	--	ENSG00000112855	HARS2	upstream
XLOC_185773	--	ENSG00000113141	IK	upstream
XLOC_185773	--	ENSG00000213523	SRA1	upstream
XLOC_185773	--	ENSG00000113119	TMCO6	upstream
XLOC_185773	--	ENSG00000120314	WDR55	upstream
XLOC_185773	--	ENSG00000146007	ZMAT2	upstream
XLOC_185773	--	ENSG00000131503	ANKHD1	downstream
XLOC_185773	--	ENSG00000254996	ANKHD1-EIF4EBP3	downstream
XLOC_185773	--	ENSG00000170458	CD14	downstream
XLOC_185773	--	ENSG00000256453	DND1	downstream
XLOC_185773	--	ENSG00000243056	EIF4EBP3	downstream
XLOC_185773	--	ENSG00000170445	HARS	downstream
XLOC_185773	--	ENSG00000131495	NDUFA2	downstream
XLOC_185773	--	ENSG00000176087	SLC35A4	downstream

C

Top10 lincRNAs with their nearby DE mRNAs

LncRNA_ID	Gene Symbol	log2FoldChange	mRNA_Gene_Id	Nearby Gene Symbol
LNC_005556	--	10.07097	ENSG00000254709	IGLL5
LNC_008045	--	9.83833	ENSG00000164821、ENSG00000164822、ENSG00000206047、ENSG00000239839、ENSG00000206047、ENSG00000164816、ENSG00000240247	DEFA4、DEFA6、DEFA1、DEFA3、DEFA5、DEFA1B、IFI44L
LNC_000788	--	9.21949	ENSG00000137959、ENSG00000122420、ENSG00000137965	IFI44L、PTGFR、IFI44
LNC_005568	--	9.21506	ENSG00000254709	IGLL5
LNC_001775	--	9.02959	ENSG00000142082、ENSG00000185187、ENSG00000177963、ENSG00000185627、ENSG00000184363、ENSG00000142102、ENSG00000174885、ENSG00000206013、ENSG00000142089、ENSG00000185201、ENSG00000185885、ENSG00000182272	SIRT3、SIGIRR、RIC8A、PSMD13、PKP3、PGGHG、NLRP6、IFITM5、IFITM3、IFITM2、IFITM1、B4GALNT4
LNC_006988	--	8.99495	ENSG00000170469、ENSG00000170482、ENSG00000120725、ENSG00000228672、ENSG00000120727、ENSG00000170476、ENSG00000015479、ENSG00000170464、	SPATA24、SLC23A1、SIL1、PROB1、PAIP2、MZB1、MATR3、DNAJC18
LNC_008046	--	8.40640	ENSG00000164821、ENSG00000164822、ENSG00000206047、ENSG00000239839、ENSG00000164816、ENSG00000240247	DEFA4、DEFA6、DEFA1、DEFA3、DEFA5、DEFA1B
LNC_003480	--	7.53459	ENSG00000140830、ENSG00000118557、ENSG00000277481、ENSG00000261701、ENSG00000257017、ENSG00000140829、ENSG00000102967	TXNL4B、PMFBP1、PKD1L3、HPR、HP、DHX38、DHODH
LNC_000783	--	7.24037	ENSG00000137959、ENSG00000122420、ENSG00000137965	IFI44L、PTGFR、IFI44
LNC_005572	--	7.15201	ENSG00000254709	IGLL5

D

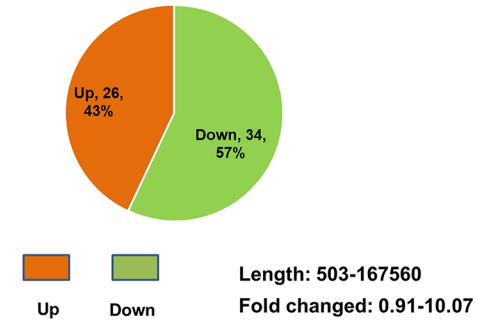

E

Top 10 antisense lncRNAs with their nearby DE mRNAs

LncRNA_ID	Gene Symbol	log2FoldChange	mRNA_Gene_Id	Nearby Gene Symbol
LNC_005556	--	10.07097	ENSG00000254709	IGLL5
LNC_005568	--	9.21506	ENSG00000254709	IGLL5
LNC_005572	--	7.152008	ENSG00000254709	IGLL5
LNC_000791	--	6.40693	ENSG00000137959、ENSG00000122420、ENSG00000137965	IFI44L、PTGFR、IFI44
LNC_008449	--	5.51637	ENSG00000214654、ENSG00000119402、ENSG00000214654、ENSG00000106780、ENSG00000119402	B3GNT10、FBXW2、B3GNT10、MEGF9、FBXW2
ENST00000650004	LUCAT1	4.36503	ENSG00000113369、ENSG00000164199	ARRDC3、ADGRV1
ENST00000510087.5	CTC-358I24.1	4.15677	ENSG00000164180	TMEM161B
LNC_005566	--	3.70439	ENSG00000254709	IGLL5
ENST00000625883.1	CDR1-AS	3.69151	ENSG00000184258	CDR1
ENST00000426275.1	RP11-439A17.10	3.63169	ENSG00000188610、ENSG00000171943、ENSG00000198019	FAM72B、SRGAP2C、FCGR1B

Fig. 7 Analysis of differentially expressed (DE) lncRNAs and their nearby DE mRNAs. (**A**) The number of lincRNAs that had nearby coding genes (distance between the lncRNA and coding gene < 100 kb) is shown in a pie chart. (**B**) *XLOC_185773* had 15 coding genes. (**C**) The top 10 lincRNAs (according to fold change) with their nearby coding genes are displayed. (**D**) The number of antisense lncRNAs with nearby coding genes is shown in a pie chart. (**E**) The top 10 antisense lncRNAs (according to fold change) with their nearby coding genes are displayed

IGLL5 in SLE may dependent on *LNC_005556*. These findings provide a novel approach to understanding the pathogenesis of SLE in terms of lncRNAs and their associated nearby coding genes. Furthermore, we analyzed the correlations between the levels of lncRNAs (*LNC_005556* or *XLOC_185773)* and the clinical indicators of patients (Additional file 15). The results revealed that *LNC_005556* shows a negative correlation with the occurrence of lupus nephritis, and *XLOC_185773* exhibits a negative correlation with the number of peripheral blood lymphocytes, which further substantiates that *LNC_005556* and *XLOC_185773* may play significant roles in the pathogenesis of SLE.

Discussion

lncRNAs play a crucial biological role in maintaining cell and tissue homeostasis [22–24]. To investigate the contribution of lncRNAs and their nearby mRNAs to the pathogenesis of SLE, we analyzed the differential expression of lncRNAs and their nearby mRNAs between a SLE group and a healthy group. Our analysis revealed 419 DE lncRNAs with 241 upregulated and 178 downregulated. Among these, *LNC_005556* was the most significantly

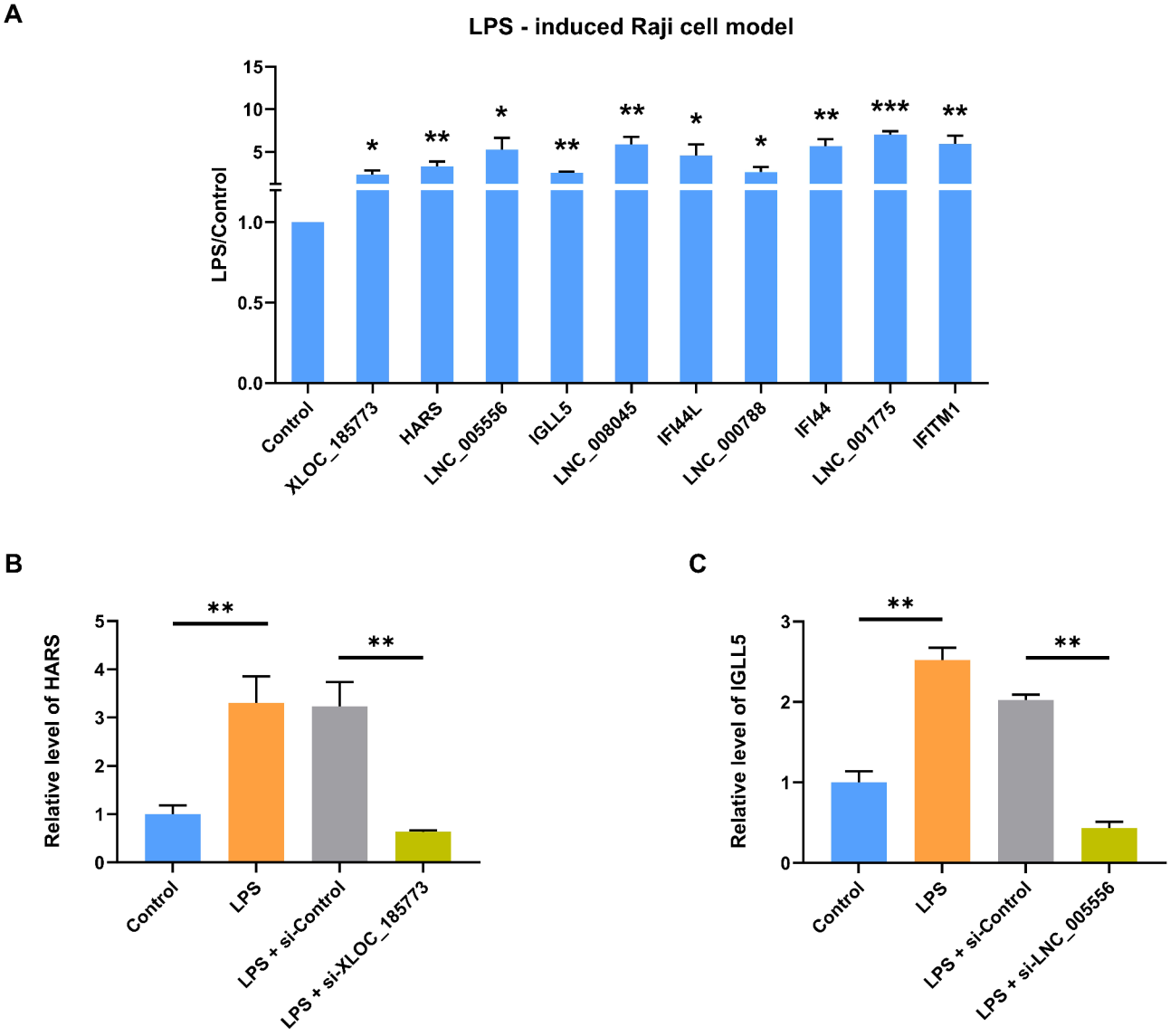

Fig. 8 Regulatory role of long non-coding RNAs (lncRNAs) on their neighboring coding genes in the Raji cell model. (**A**) Expression patterns of lncRNAs and their neighboring coding genes in the Raji model following lipopolysaccharide (LPS) induction ($n=6$). (**B**) Expression levels of *HARS* in the Raji cell model upon silencing of *XLOC_185773* ($n=6$). (**C**) Expression levels of *IGLL5* in the Raji cell model upon silencing of *LNC_005556* ($n=6$). *$p<0.05$, **$p<0.01$, ***$p<0.001$

upregulated lncRNA, and *LNC_000099* was the most significantly downregulated lncRNA, both of which were previously undescribed genes. We also identified 337 DE nearby mRNAs of these DE lncRNAs, with 234 upregulated and 103 downregulated.

The nearby mRNA with the most obvious upregulation was *LTF*, which is an iron-binding glycoprotein with immunomodulatory function and antimicrobial activity [25]. Recurrent infection in SLE patients may upregulate *LTF*. *LTF* or the immune response against *LTF* may associate with the onset of IgG4-related diseases through the activation of innate immune response and fibroblast proliferation [26, 27]. However, to our knowledge, we newly identified its relevance to SLE pathogenesis. Additionally, the most significantly downregulated nearby mRNA was *CIRBP*. By binding to the target mRNA 3'-UTR, it regulates mRNA-stability, promotes translation, responds to various stresses, and helps cells adapt to new environmental conditions [28]. *CIRBP* plays a crucial role in regulating DNA double strand break (DSB) repair. Enhanced sensitivity to γ rays was observed in *CIRBP*-deficient cells [29]. *CIRBP* not only participates in the anti-apoptotic process under mild hypothermia, but also protects against cell senescence induced by ultraviolet radiation and hypoxia [30]. In HaCaT cells, the knockdown of CIRBP enhanced UVB-induced PARP cleavage

and caspase 3 activation, thereby confirming the role of CIRBP in inhibiting UVB-induced apoptosis of keratinocytes [31]. Current studies have shown that CIRBP expression is associated with reduced susceptibility to UV-mediated apoptosis in cells by modulating stress response and apoptosis pathways [32–36]. Our study revealed that *CIRBP* was downregulated in SLE patients, which may lead to instability of stress-related mRNA and damaged DNA double strands. This can result in the generation of the autoantigens that participate in the pathogenesis of SLE. Therefore, we hypothesize that the downregulation of *CIRBP* in SLE patients may explain why ultraviolet radiation is one of the susceptibility factors of SLE. Moreover, *CIRBP* protects neurons against amyloid toxicity through antioxidant and anti-apoptotic pathways [37]. However, whether it is involved in neurological changes in SLE patients remains to be determined.

The immune effector process was identified as the most significant upregulated term in the GO analysis. Participating genes included *IFIT1*, *IFIT2*, *SIGLEC14*, *S100A8*, *S100A12*, among others. *IFIT1* is positively correlated with podocyte injury in lupus nephritis [38], while *IFIT2* is significantly upregulated in the blood of SLE patients and positively correlated with SLE disease activity [39]. Sialic acid-binding Ig-like Lectin 14 (*SIGLEC14*) in monocytes is positively correlated with the SLEDAI score, anti-Sm and anti-SSB autoantibodies, and may be involved in the inflammation of SLE [40]. Elevated *S100A8* levels are observed in anti-dsDNA antibody-positive SLE patients, and *S100A12* may serve as a disease activity marker of SLE [41]. Similarly, elevated *S100A12* levels were reported in adults and children with active lupus [42, 43]. A previous study reported that upregulated genes were enriched in the term of defense and immune response in SLE patients [12], which is consistent with our findings.

Downregulated genes were enriched in the GO term of negative regulation of single-stranded viral RNA replication via double-stranded DNA intermediate. Members of the *APOBEC* family, including *APOBEC3F*, *APOBEC3G*, *APOBEC3D*, *APOBEC3H* were the main genes involved. *APOBEC*s play a crucial role in the conversion of cytosine to uracil. The downregulation of this term may lead to the accumulation of C-U mismatch and the formation of new autoantigens. Moreover, the clearance of exogenous and endogenous DNA in cells is also weakened [44, 45]. Previous studies reported that *APOBEC* is involved in the pathogenesis of SLE by generating or increasing the autoantigen load, which is recognized by the body and triggers an immune response [46].

The pertussis signaling pathway was found to be significantly upregulated. The upregulated genes included *C1qA*, *C1qB*, *C1qC*, *CXCL6*, and *CXCL8*. *C1q* is involved in the classic mechanism of complement activation in SLE [47]. *CXCL8* and *CXCL6* are the main mediators of inflammatory response. *IL8*, also known as *CXCL8*, is significantly increased in SLE patients and involved in the pathogenesis of SLE by chemotactic neutrophils [48]. Additionally, *NLRP3*, *IL1A*, *IL1β*, and *IL10* were upregulated in the pertussis signaling pathway. *NLRP3* enhances *IL1* production and plays a role in the regulation of inflammation, immune response, and apoptosis [49]. *NLRP3* and *IL1β* are significantly upregulated in macrophages and PBMCs of SLE patients [50, 51]. Interestingly, the upregulated genes *C1qA*, *C1qC*, *C1qB*, *NLRP3*, and *CXCL6* participate in the GO terms of immune effector process and protein binding, suggesting their involvement in immune responses at different stages in SLE pathogenesis. Similarly, Cheng et al. [12] reported that genes of the complement pathway were upregulated in SLE patients.

The lysosome pathway exhibited the most significant downregulation in our study. Lysosomes play a crucial role in maintaining immune homeostasis by degrading phagocytotic fragments of apoptosis. In SLE, lysosome maturation is defective, leading to the inability of macrophages to degrade immune complexes formed by IgG binding to apoptotic blebs [52]. Consequently, the downregulation of this pathway may result in the accumulation of apoptotic fragments, which act as antigens to trigger the onset of SLE [13].

By comparing our discovered DE lncRNA, mRNA, GO term or KEGG with some existing key related studies [13, 53, 54], we found that there was no overlapping part among the lncRNA, mRNA or KEGG obtained in different studies. That is to say, most lncRNAs, mRNAs or KEGG pathways in different studies are specific. The differences in these results may be related to the genetic background of the population, data source, sample selection, research design, analysis strategy or the complexity of the SLE pathological mechanism. For example, Cao et al. [13] used samples from patients in the USA, Spain, Australia and Japan, while our study focused on patients in China. Moreover, Cao et al. analyzed mRNAs, while our study examined the nearby mRNAs of differentially expressed lncRNAs. However, there is partial overlap in the GO analysis results obtained in different studies, and the GO term "Metabolic processes" was found in one previous study [53] and our study. This result indicates that the biological process of "Metabolic processes" may play an important role in the pathological mechanism of SLE. The repeated findings provide consistency and reliability for the study of the molecular mechanism of SLE.

We identified 88 lincRNAs with nearby mRNAs, among which upregulated *XLOC_185773* (LncRNA transcript id: *LNC_004051*) had the most coding genes (7 upstream genes and 8 downstream genes). Upstream *HARS2* (ENST00000448069: upregulated,

ENST00000642970: downregulated) and downstream *HARS* (ENST00000307633: upregulated) are aminoacyl-tRNA synthases, involved in the synthesis of histidine transfer RNA. Although the role of histidine transfer RNA in SLE is unclear, it is a common target of autoantibodies in the human autoimmune disease polymyositis/dermatomyositis [55]. We observed a positive correlation between the levels of *XLOC_185773* and the levels of *HARS*, and *XLOC_185773* may be involved in the pathogenesis of SLE by regulating *HARS*. In the result of the correlation analysis between *XLOC_185773* and the clinical indicators of patients, we found that *XLOC_185773* exhibits a significant negative correlation with the number of peripheral blood lymphocytes. Lymphopenia is one of the most common clinical manifestations of SLE and also one of the bases for hematological system damage in the diagnostic criteria of SLE. This result supports the hypothesis that *XLOC_185773* may be involved in the pathogenesis of SLE. Among the mRNAs near the DE lincRNAs, upregulated *DEFA* and *IFITM* genes are involved in defense functions, the innate immune system, and interferon gamma signaling pathways. Consistent with our findings, Novaes E.B.R.R. et al. observed *IFITM1* upregulation in (NZB/NZW) F1 mice [56] and in the platelets of SLE patients [57]. Cao et al. [13] also reported upregulation of *IFI44* and *IFI44L* in SLE patients, which may contribute to facial erythema and positive anti-Smith antibodies [58].

In addition, we identified upregulated *IGLL5* in SLE patients, which encodes an immunoglobulin λ like polypeptide, and was associated with three lincRNAs (*LNC_005556*, *LNC_005568*, *LNC_005572*) and four antisense lncRNAs (*LNC_005556*, *LNC_005568*, *LNC_005572*, *LNC_005566*). We found that LNC_005556 may positively regulate IGLL5, supporting the hypothesis that LNC_005556 is involved in the pathogenesis of SLE. It would be intriguing to explore whether LNC_005556 or IGLL5 could potentially serve as a potential target for SLE. Surprisingly, however, we discovered that LNC_005556 is negatively correlated with the occurrence of lupus nephritis, indicating that different regulatory mechanisms may be involved in the process of lupus nephritis occurrence, or additional factors that are not fully captured by the relationship between LNC_005556 and IGLL5. Hence, identifying other potential downstream targets of LNC_005556 that may be potentially relevant to the occurrence of lupus nephritis might be crucial for understanding the heterogeneity of SLE and its various clinical manifestations. Although upregulated *IGLL5* is reported to be involved in the pathogenesis of rheumatoid arthritis [59], we report for the first time its involvement in SLE pathogenesis. On one hand, we recognize the necessity of further research to comprehensively understand the specificity of *IGLL5* in SLE pathogenesis. On the other hand, further investigating the abnormal expression of *IGLL5* in different rheumatic diseases will also contribute to exploring the possibility of *IGLL5* becoming a non-specific indicator for rheumatic diseases.

The advantages of this study are as follows: Firstly, it employs high-throughput sequencing technology to conduct a comprehensive expression analysis of lncRNAs in SLE patients, uncovering some novel lncRNAs. Secondly, the findings possess strong clinical relevance as they explore the potential correlations with the disease activity. Finally, it provides data integrity by offering abundant clinical information and gene expression data, establishing a valuable database for future research on SLE. The limitations include: Firstly, the study population mainly from a specific region which may impact the universality of the results. Secondly, si-*CIRBP* studies and UV irradiation experiments were not conducted in the Raji cell line. Finally, functional verification of the identified DE lncRNAs is insufficient. Future research directions involve specifically validating the expressions of DE lncRNAs in B cells from SLE patients, and increasing the sample size to comprehensively investigate the underlying mechanisms of the DE lncRNAs in SLE.

Conclusions

Utilizing high-throughput sequencing, we identified DE lncRNAs and their nearby DE mRNAs in SLE, which may contribute to explaining the molecular mechanisms linked to susceptibility factors such as lupus photosensitivity and infections. Our results underscore the significance of the complement system and inflammatory mediators, including *C1qA*, *C1qB*, *C1qC*, *NLRP3*, and *CXCL6*, in SLE, alongside an upregulation of the stress defense pathway against infection in patients. Additionally, analysis of genes adjacent to lincRNAs highlighted *HARS*, *DEFA*, *IFITM*, and *IGLL5* as potential targets for further exploration of SLE pathogenesis. Notably, we identified two lncRNAs in SLE patients, *XLOC_185773* and *LNC_005556*, which are significantly upregulated and may regulate *HARS* and *IGLL5*, respectively. Furthermore, a negative correlation was observed between the expression of *XLOC_185773* and the reduction of peripheral blood lymphocytes, as well as between *LNC_005556* and lupus nephritis. These findings provide deeper insights into SLE pathology and propose potential biomarkers for early diagnosis and treatment, warranting additional investigation.

Abbreviations

ACR	American Society of Rheumatology
APOBEC	Apolipoprotein B mRNA editing enzyme catalytic
ARID1A	AT-rich interaction domain 1 A
aCL-IgA	Anticardiolipin IgA Antibodies
aCL-IgM	Anticardiolipin IgM Antibodies
aCL-IgG	Anticardiolipin IgG Antibodies

anti-dsDNA	Anti-double stranded DNA antibody
BP	Biological process
CC	Cellular component
CIRBP	Cold inducible RNA binding protein
CTRL	Control
CXCL	C-X-C motif chemokine ligand
DE	Differentially expressed
DEFA	Defensin Alpha
ESR	Erythrocyte Sedimentation Rate
FC	Fold change
FPKM	Fragments per kilobase of exon model per million mapped fragments
GO	Gene ontology
HARS	Histidyl-tRNA synthetase
HBB	Hemoglobin subunit beta
IFI	Interferon induced protein
IFIT	Interferon induced protein with tetratricopeptide repeats
IFITM	Interferon induced transmembrane protein
IFN	Interferon
IGLL5	Immunoglobulin lambda like polypeptide 5
IL	Interleukin
KEGG	Kyoto encyclopedia of genes and genomes
LMBRD2	LMBR1 domain containing 2
lincRNA	Long intergenic non-coding RNA
lncRNA	Long non-coding RNA
LPS	Lipopolysaccharide
LTF	Lactotransferrin
LY	Lymphocyte Count
MF	Molecular function
mRNA	Messenger RNA
NLRP3	NLR Family Pyrin Domain Containing 3
PBMC	Peripheral blood mononuclear cells
PHACTR4	Phosphatase and actin regulator 4
qRT-PCR	Quantitative real-time PCR
S100A	S100 calcium binding protein A
SIGLEC14	Sialic acid-binding Ig-like Lectin 14
si-RNA	Small interference RNA
SLE	Systemic lupus erythematosus
SLEDAI	Systemic lupus erythematosus disease activity index 2000
SPG7	SPG7 Matrix AAA Peptidase Subunit
TEC	Tec Protein Tyrosine Kinase
WBC	White Blood Cell Count

Supplementary Information

The online version contains supplementary material available at https://doi.org/10.1186/s13075-025-03510-1.

Additional file 1.docx: Clinical information of the patients.

Additional file 2.docx: Detailed clinical information for the 50 patients with Systemic Lupus Erythematosus (SLE).

Additional file 3.pdf: Age and Gender Distribution in the Healthy Control Group (A) and the Systemic Lupus Erythematosus (SLE) Group (B). This figure depicts the demographic composition of these two groups, where orange bars signify female participants and blue bars represent male participants. The numerical values superimposed on the bars match the percentage of females in each specific age range.

Additional file 4.docx: The sequence of the qRT-PCR primers.

Additional file 5.docx: Top 20 significantly upregulated GO terms of biological process.

Additional file 6.docx: Top 20 significantly upregulated GO terms of cellular component.

Additional file 7.docx: Top 20 significantly upregulated GO terms of molecular function.

Additional file 8.docx: Top 20 significantly downregulated GO terms of biological process.

Additional file 9.docx: Top 20 significantly downregulated GO terms of cellular component.

Additional file 10.docx: Top 20 significantly downregulated GO terms of molecular function.

Additional file 11.pdf: Pertussis pathway. The red squares represent the DE mRNAs.

Additional file 12.tif: The analysis on the FPKMs of ***HARS***, ***HARS2*** or ***XLOC_185773***. (A) The FPKMs of ***HARS*** (ENST00000307633). (B) The FPKMs of ***HARS2*** (ENST00000448069). (C) The FPKMs of ***HARS2*** (ENST00000642970) (D) The FPKMs of ***XLOC_185773*** (LNC_004051). * p-adjust < 0.05, ** p-adjust < 0.01, *** p-adjust < 0.001. (E) The correlation analysis between the mRNAs (***HARS***, ***HARS2***) and the lncRNA (***XLOC_185773***).

Additional file 13.tif: The analysis on the FPKMs of ***IGLL5*** or ***XLOC_145172***. (A) The FPKMs of ***IGLL5*** (ENST00000532223). (B) The FPKMs of ***IGLL5*** (ENST00000531372). (C) The FPKMs of ***IGLL5*** (ENST000005268893) (D) The FPKMs of ***XLOC_145172*** (LNC_005556). * p-adjust < 0.05, ** p-adjust < 0.01, *** p-adjust < 0.001. (E) The correlation analysis between the mRNAs (***IGLL5***) and the lncRNA (***XLOC_145172***).

Additional file 14.tif: Histogram illustrating the gene expression levels in peripheral blood mononuclear cells (PBMCs) of healthy human subjects, as determined by single-cell sequencing data. The data source for this analysis is available from EMBL's European Bioinformatics Institute (website: http://www.ebi.ac.uk/gxa/experiments/E-MTAB-3827/Downloads?specific=true%26geneQuery=%255B%257B%2522value%2522%253A%2522ensg00000106799%2522%257D%255D%26filterFactors=%257B%257D%26cutoff=%257B%2522value%2522%253A0.5%257D%26unit=%2522FPKM%2522).

Additional file 15.pdf: Correlation analysis of RNA levels and clinical manifestations in the SLE cohort. A Spearman's rank correlation heatmap shows the correlation between the FPKM expression levels of mRNAs (***HARS*** and ***IGLL5***) and their co-located lncRNA (***XLOC_185773*** and ***LNC_005556***) with patients' clinical information. The size of the circles represents the absolute value of the correlation coefficient; red circles indicate a positive correlation coefficient, denoting a positive correlation, and blue circles indicate a negative correlation coefficient, indicating a negative correlation. Asterisks within the circles signify significant correlation between the two variables. *$p < 0.05$. Abbreviations: LN (Lupus Nephritis), SLEDAI (Systemic Lupus Erythematosus Disease Activity Index), C3 (Complement Component 3), C4 (Complement Component 4), CRP (C-reactive Protein), ESR (Erythrocyte Sedimentation Rate), WBC (White Blood Cell Count), LY (Lymphocyte Count), anti-dsDNA (Anti-double stranded DNA antibody), aCL-IgA (aCL-IgA, Anticardiolipin IgA Antibodies), aCL-IgM (Anticardiolipin IgM Antibodies), aCL-IgG (Anticardiolipin IgG Antibodies).

Acknowledgements

The authors thank all the patients who have participated in the study. The authors also thank Mr. Yingjie Li and his colleagues of Novogene Co. Ltd (Beijing) for their assistance in data processing.

Author contributions

TL collected the clinical samples, contributed to experiments, and wrote the manuscript; MY performed experiments, did the statistical analysis, and created figures and tables; XF and XZ collected the clinical samples and analyzed the clinical information; YX, LC, and ZG are involved in qRT-PCR experiments; LZ completed the manuscript; XW designed the study, analyzed the data, and revised the manuscript; all of the authors read and approved the manuscript.

Funding

This work was supported by the Department of Science and Technology of Jilin Province, China [grant number 20210204174YY]; the Starting Fund of the First Hospital of Jilin University [grant number 04032690001]; First Hospital of Jilin University [grant number JDYY14202322]; Science and Technology Department of Jilin Province [grant number YDZJ202201ZYTS018]; Jilin University "The Bethune Grant" [grant number 2023B07]. The funders had no role in study design, data collection and analysis, decision to publish, or preparation of the manuscript.

Data availability
The datasets generated and/or analyzed during the current study are available in the GEO repository (accession number: GSE211700, https://www.ncbi.nlm.nih.gov/geo/query/acc.cgi?acc=GSE211700).

Declaration

Ethics approval and consent to participate
Ethics approval for this study was provided by the Institutional Medical Ethics Review Board of the First Hospital of Jilin University (reference number: 2017-087) and all procedures were in compliance with the Declaration of Helsinki.

Consent for publication
Not applicable.

Competing interests
The authors declare no competing interests.

Received: 7 May 2024 / Accepted: 18 February 2025
Published online: 01 March 2025

References

1. Rees F, Doherty M, Grainge MJ, Lanyon P, Zhang W. The worldwide incidence and prevalence of systemic lupus erythematosus: a systematic review of epidemiological studies. Rheumatology (Oxford). 2017;56(11):1945–61.
2. Hart PH, Norval M, Byrne SN, Rhodes LE. Exposure to ultraviolet radiation in the modulation of human diseases. Annu Rev Pathol. 2019;14:55–81.
3. Quaglia M, Merlotti G, De Andrea M, Borgogna C, Cantaluppi V. Viral infections and systemic lupus erythematosus: new players in an old story. Viruses. 2021;13(2).
4. Chyuan IT, Tzeng HT, Chen JY. Signaling pathways of type I and type III interferons and targeted therapies in systemic lupus erythematosus. Cells. 2019;8(9).
5. Shao WH, Cohen PL. Disturbances of apoptotic cell clearance in systemic lupus erythematosus. Arthritis Res Ther. 2011;13(1):202.
6. Leffler J, Bengtsson AA, Blom AM. The complement system in systemic lupus erythematosus: an update. Ann Rheum Dis. 2014;73(9):1601–6.
7. Ransohoff JD, Wei Y, Khavari PA. The functions and unique features of long intergenic non-coding RNA. Nat Rev Mol Cell Biol. 2018;19(3):143–57.
8. Zou Y, Xu H. Involvement of long noncoding RNAs in the pathogenesis of autoimmune diseases. J Transl Autoimmun. 2020;3:100044.
9. Ponting CP, Oliver PL, Reik W. Evolution and functions of long noncoding RNAs. Cell. 2009;136(4):629–41.
10. Ebisuya M, Yamamoto T, Nakajima M, Nishida E. Ripples from neighbouring transcription. Nat Cell Biol. 2008;10(9):1106–13.
11. Jiang B, Yuan Y, Yi T, Dang W. The roles of antisense long noncoding RNAs in tumorigenesis and development through Cis-Regulation of neighbouring genes. Biomolecules. 2023;13(4).
12. Cheng Q, Chen M, Chen X, Chen X, Jiang H, Wu H, et al. Novel long Non-coding RNA expression profile of peripheral blood mononuclear cells reveals potential biomarkers and regulatory mechanisms in systemic lupus erythematosus. Front Cell Dev Biol. 2021;9:639321.
13. Cao H, Li D, Lu H, Sun J, Li H. Uncovering potential LncRNAs and nearby mRNAs in systemic lupus erythematosus from the gene expression omnibus dataset. Epigenomics. 2019;11(16):1795–809.
14. Gao M, Wang K, Yang M, Meng F, Lu R, Zhuang H, et al. Transcriptome analysis of Bronchoalveolar lavage fluid from children with Mycoplasma pneumoniae pneumonia reveals natural killer and T Cell-Proliferation responses. Front Immunol. 2018;9:1403.
15. Wang K, Gao M, Yang M, Meng F, Li D, Lu R, et al. Transcriptome analysis of Bronchoalveolar lavage fluid from children with severe Mycoplasma pneumoniae pneumonia reveals novel gene expression and immunodeficiency. Hum Genomics. 2017;11(1):4.
16. Yang M, Wang P, Liu T, Zou X, Xia Y, Li C, et al. High throughput sequencing revealed enhanced cell cycle signaling in SLE patients. Sci Rep. 2023;13(1):159.
17. Langmead B, Salzberg SL. Fast gapped-read alignment with bowtie 2. Nat Methods. 2012;9(4):357–9.
18. Pertea M, Kim D, Pertea GM, Leek JT, Salzberg SL. Transcript-level expression analysis of RNA-seq experiments with HISAT, stringtie and ballgown. Nat Protoc. 2016;11(9):1650–67.
19. Frazee AC, Sabunciyan S, Hansen KD, Irizarry RA, Leek JT. Differential expression analysis of RNA-seq data at single-base resolution. Biostatistics. 2014;15(3):413–26.
20. Yuan Y, Yang M, Wang K, Sun J, Song L, Diao X, et al. Excessive activation of the TLR9/TGF-beta1/PDGF-B pathway in the peripheral blood of patients with systemic lupus erythematosus. Arthritis Res Ther. 2017;19(1):70.
21. Faghihi MA, Wahlestedt C. Regulatory roles of natural antisense transcripts. Nat Rev Mol Cell Biol. 2009;10(9):637–43.
22. Moran VA, Perera RJ, Khalil AM. Emerging functional and mechanistic paradigms of mammalian long non-coding RNAs. Nucleic Acids Res. 2012;40(14):6391–400.
23. Li LJ, Zhao W, Tao SS, Li J, Xu SZ, Wang JB, et al. Comprehensive long non-coding RNA expression profiling reveals their potential roles in systemic lupus erythematosus. Cell Immunol. 2017;319:17–27.
24. Yao RW, Wang Y, Chen LL. Cellular functions of long noncoding RNAs. Nat Cell Biol. 2019;21(5):542–51.
25. Actor JK, Hwang SA, Kruzel ML. Lactoferrin as a natural immune modulator. Curr Pharm Des. 2009;15(17):1956–73.
26. Tsuboi H, Honda F, Takahashi H, Ono Y, Abe S, Kondo Y, et al. Pathogenesis of IgG4-related disease. Comparison with Sjogren's syndrome. Mod Rheumatol. 2020;30(1):7–16.
27. Tsuboi H, Nakai Y, Iizuka M, Asashima H, Hagiya C, Tsuzuki S, et al. DNA microarray analysis of labial salivary glands in IgG4-related disease: comparison with Sjogren's syndrome. Arthritis Rheumatol. 2014;66(10):2892–9.
28. Zhong P, Peng J, Yuan M, Kong B, Huang H. Cold-inducible RNA-binding protein (CIRP) in inflammatory diseases: molecular insights of its associated signalling pathways. Scand J Immunol. 2021;93(1):e12949.
29. Chen JK, Lin WL, Chen Z, Liu HW. PARP-1-dependent recruitment of cold-inducible RNA-binding protein promotes double-strand break repair and genome stability. Proc Natl Acad Sci U S A. 2018;115(8):E1759–68.
30. Liao Y, Tong L, Tang L, Wu S. The role of cold-inducible RNA binding protein in cell stress response. Int J Cancer. 2017;141(11):2164–73.
31. Liao Y, Feng J, Zhang Y, Tang L, Wu S. The mechanism of CIRP in Inhibition of keratinocytes growth arrest and apoptosis following low dose UVB radiation. Mol Carcinog. 2017;56(6):1554–69.
32. Corre M, Lebreton A. Regulation of cold-inducible RNA-binding protein (CIRBP) in response to cellular stresses. Biochimie. 2024;217:3–9.
33. Kim YM, Hong S. Controversial roles of cold–inducible RNA–binding protein in human cancer (Review). Int J Oncol. 2021;59(5).
34. Han J, Zhang Y, Ge P, Dakal TC, Wen H, Tang S, et al. Exosome-derived CIRP: an amplifier of inflammatory diseases. Front Immunol. 2023;14:1066721.
35. Zhong P, Huang H. Recent progress in the research of cold-inducible RNA-binding protein. Future Sci OA. 2017;3(4):FSO246.
36. Sheikh MS, Carrier F, Papathanasiou MA, Hollander MC, Zhan Q, Yu K, et al. Identification of several human homologs of hamster DNA damage-inducible transcripts. Cloning and characterization of a novel UV-inducible cDNA that codes for a putative RNA-binding protein. J Biol Chem. 1997;272(42):26720–6.
37. Su F, Yang S, Wang H, Qiao Z, Zhao H, Qu Z. CIRBP ameliorates neuronal amyloid toxicity via antioxidative and antiapoptotic pathways in primary cortical neurons. Oxid Med Cell Longev. 2020;2020:2786139.
38. Hu W, Niu G, Li H, Gao H, Kang R, Chen X, et al. The association between expression of IFIT1 in podocytes of MRL/lpr mice and the renal pathological changes it causes: an animal study. Oncotarget. 2016;7(47):76464–70.
39. Zhao ZY, Yang NP, Huang XY, Min L, Liu XX, Zhang J, et al. [Interferon-inducible genes 2', 5'-ollgoadenylate synthetase-like and tetratricopeptide repeats 2 are correlated with clinical features of patients with systemic lupus erythematosus]. Sichuan Da Xue Xue Bao Yi Xue Ban. 2010;41(2):247–51.
40. Thornhill SI, Mak A, Lee B, Lee HY, Poidinger M, Connolly JE, et al. Monocyte Siglec-14 expression is upregulated in patients with systemic lupus erythematosus and correlates with lupus disease activity. Rheumatology (Oxford). 2017;56(6):1025–30.
41. Tyden H, Lood C, Gullstrand B, Jonsen A, Ivars F, Leanderson T, et al. Pro-inflammatory S100 proteins are associated with glomerulonephritis and anti-dsDNA antibodies in systemic lupus erythematosus. Lupus. 2017;26(2):139–49.
42. Davies JC, Midgley A, Carlsson E, Donohue S, Bruce IN, Beresford MW et al. Urine and serum S100A8/A9 and S100A12 associate with active lupus nephritis and May predict response to rituximab treatment. RMD Open. 2020;6(2).

43. Donohue SJ, Midgley A, Davies JC, Wright RD, Bruce I, Beresford MW, et al. Differential analysis of serum and urine S100 proteins in juvenile-onset systemic lupus erythematosus (jSLE). Clin Immunol. 2020;214:108375.
44. Stenglein MD, Burns MB, Li M, Lengyel J, Harris RS. APOBEC3 proteins mediate the clearance of foreign DNA from human cells. Nat Struct Mol Biol. 2010;17(2):222–9.
45. Suspene R, Mussil B, Laude H, Caval V, Berry N, Bouzidi MS, et al. Self-cytoplasmic DNA upregulates the mutator enzyme APOBEC3A leading to chromosomal DNA damage. Nucleic Acids Res. 2017;45(6):3231–41.
46. Roth SH, Danan-Gotthold M, Ben-Izhak M, Rechavi G, Cohen CJ, Louzoun Y, et al. Increased RNA editing May provide a source for autoantigens in systemic lupus erythematosus. Cell Rep. 2018;23(1):50–7.
47. Song D, Guo WY, Wang FM, Li YZ, Song Y, Yu F, et al. Complement alternative pathways activation in patients with lupus nephritis. Am J Med Sci. 2017;353(3):247–57.
48. Mao YM, Zhao CN, Liu LN, Wu Q, Dan YL, Wang DG, et al. Increased Circulating interleukin-8 levels in systemic lupus erythematosus patients: a meta-analysis. Biomark Med. 2018;12(11):1291–302.
49. Li Z, Guo J, Bi L. Role of the NLRP3 inflammasome in autoimmune diseases. Biomed Pharmacother. 2020;130:110542.
50. Yang CA, Huang ST, Chiang BL. Sex-dependent differential activation of NLRP3 and AIM2 inflammasomes in SLE macrophages. Rheumatology (Oxford). 2015;54(2):324–31.
51. Furini F, Giuliani AL, Parlati ME, Govoni M, Di Virgilio F, Bortoluzzi A. P2X7 Receptor Expression in Patients With Serositis Related to Systemic Lupus Erythematosus. Front Pharmacol. 2019;10:435.
52. Monteith AJ, Kang S, Scott E, Hillman K, Rajfur Z, Jacobson K, et al. Defects in lysosomal maturation facilitate the activation of innate sensors in systemic lupus erythematosus. Proc Natl Acad Sci U S A. 2016;113(15):E2142–51.
53. Ye H, Wang X, Wang L, Chu X, Hu X, Sun L, et al. Full high-throughput sequencing analysis of differences in expression profiles of long noncoding RNAs and their mechanisms of action in systemic lupus erythematosus. Arthritis Res Ther. 2019;21(1):70.
54. Luo Q, Li X, Xu C, Zeng L, Ye J, Guo Y, et al. Integrative analysis of long noncoding RNAs and messenger RNA expression profiles in systemic lupus erythematosus. Mol Med Rep. 2018;17(3):3489–96.
55. Ascherman DP, Oriss TB, Oddis CV, Wright TM. Critical requirement for professional apcs in eliciting T cell responses to novel fragments of histidyl-tRNA synthetase (Jo-1) in Jo-1 antibody-positive polymyositis. J Immunol. 2002;169(12):7127–34.
56. Novaes EBRR, Xander P, Perez EC, Maricato JT, Laurindo MF, De Lorenzo BH, et al. Gene expression in B-1 cells from lupus-prone mice. Immunol Invest. 2014;43(7):675–92.
57. Lood C, Amisten S, Gullstrand B, Jonsen A, Allhorn M, Truedsson L, et al. Platelet transcriptional profile and protein expression in patients with systemic lupus erythematosus: up-regulation of the type I interferon system is strongly associated with vascular disease. Blood. 2010;116(11):1951–7.
58. Shen M, Duan C, Xie C, Wang H, Li Z, Li B, et al. Identification of key interferon-stimulated genes for indicating the condition of patients with systemic lupus erythematosus. Front Immunol. 2022;13:962393.
59. Wu B, He Y, Yang D, Liu RX. Identification of hub genes and therapeutic drugs in rheumatoid arthritis patients. Clin Rheumatol. 2021;40(8):3299–309.

Publisher's note